Submitted to small NANO MICRO

DOI: 10.1002/smll.201300975

Solvent-Cast Three-Dimensional Printing of Multifunctional Microsystems

*Shuang-Zhuang Guo, Frédérick Gosselin, Nicolas Guerin, Anne-Marie Lanouette, Marie-Claude Heuzey and Daniel Therriault**

[*] Prof. D. Therriault, S. Z. Guo, Prof. F. Gosselin, N. Guerin and A. M. Lanouette
Laboratory of Multiscale Mechanics, Mechanical Engineering Department
Center for Applied Research on Polymers and composites (CREPEC)
École Polytechnique de Montréal
C.P. 6079, succ. Centre-Ville, Montreal, QC H3C 3A7 (Canada)
E-mail: daniel.therriault@polymtl.ca
Prof. M. C. Heuzey
Chemical Engineering Department
Center for Applied Research on Polymers and composites (CREPEC)
École Polytechnique de Montréal
C.P. 6079, succ. Centre-Ville, Montreal, QC H3C 3A7 (Canada)

Keywords: Microfabrication, Solvent-cast, Thermoplastics, Polylactide, 3-D Printing

Three-dimensional (3-D) structures fabricated from polymers and their nanocomposites may find widespread technological applications as sensors,[1-3] microvascular networks,[4, 5] self-healing materials,[6-9] and tissue engineering scaffolds.[10-12] Theses applications either require, or could benefit from, the ability to pattern micro-sized features in complex 3-D architectures. Several strategies and technologies have recently emerged to rapidly and cost-effectively fabricate thermoplastic polymer-based 3-D microdevices. For example, fused deposition modeling (FDM) stands out as the most popular procedure to manufacture 3-D products with a spatial resolution down to 45 μm.[13] However, the thermal degradation caused by high processing temperatures and the high viscosity of most polymer melts may prevent the application of this technique to be compatible with

nanocomposite devices, since nanoparticles can significantly increase material viscosity. Also, electrospinning has been used to produce fiber-based polymer structures with fiber diameters ranging from ~100 nm to ~300 μm[14-16] but is limited in terms of 3-D structure complexity.[14]

Direct-write (DW) assembly is a 3-D printing technique that employs a computer-controlled translation stage, which moves an ink-deposition nozzle, to create materials with controlled architecture and composition.[17] This technique requires specific ink rheological and viscoelastic properties. First, the ink viscosity should be low to moderate to facilitate its extrusion through a capillary micronozzle under applied pressure. Second, the rigidity of the filament after extrusion must quickly increase for shape retention. Many ink materials have been employed such as organic fugitive ink,[18] concentrated polyelectrolyte complexes,[19] colloidal suspensions,[20-22] hydrogels[23, 24] and thermoset polymers.[25] These inks solidify through different mechanisms such as viscoelastic recoil,[18] coagulation in reservoir,[19] suppression of repulsive forces,[20] and UV polymerization.[23-25] Thermoplastic polymers have also been used in the direct write technique (fused deposition) due to their rigidity increase after the temperature-triggered phase transition from melt to solid,[13] however this method exhibited limited control of the 3-D printed feature geometries.

The solvent-cast direct-write (SC-DW) fabrication method presented in this study was developed to fabricate 3-D geometries at room temperature in a freeform fashion with dissolvable thermoplastic polymers (see **Scheme 1**). The method consists of the

robotically controlled micro-extrusion of a concentrated polymer solution ink filament, combined with rapid solvent evaporation after the filament exits the micronozzle. Under applied pressure, the polymer solution, which undergoes capillary shear flow inside the micronozzle, relaxes its stresses upon exiting the nozzle. As the solvent evaporates post extrusion, the diameter of the filament decreases and its rigidity gradually increases with time due to a locally higher polymer concentration. This rigidity gradient enables the creation of self-supporting curved shape by changing the moving path of the extrusion nozzle, in which the filament bending occurs in the low rigidity zone of the newly extruded material. After most of the solvent evaporation, the rigidity of the extruded filament changes from fluid-like to solid-like, which facilitates the shape retention of the deposited self-supporting features. This 3-D printing process enables the creation of different multifunctional microsystems featuring complex geometries.

For successful solvent-cast direct writing of 3-D freeform structures, the selected solvent and the polymer concentration in the solution have to be set to ensure proper ink rheological behavior while providing a fast solvent evaporation. Then, the velocity of the extrusion nozzle and the applied pressure on the polymer solution must be tailored to achieve the desired material linear flow rate. In this initial demonstration, the thermoplastic used was polylactide (PLA), a polymer derived from renewable resources, and the solvent was dichloromethane (DCM, boiling point = 39.6 ºC) due to of its fast evaporation and good PLA dissolvability.

The viscoelastic properties of the polymer solution, which were tailored by varying

the polymer concentration, determined its flowing behavior inside the nozzle and the initial rigidity of the extruded filament. A polymer solution with high viscosity required a high applied pressure during the extrusion step. On the other hand, a lower viscosity solution flowed from the nozzle more easily; however the resulting filament needed more time to dry since it contained more solvent. Because of the solubility limitation of PLA in DCM at room temperature, the maximum PLA concentration studied in this project was 30 wt%; solutions of 20 and 25 wt% PLA were also investigated. The process-related apparent viscosity of the three PLA solutions was determined by capillary flow analysis in the nozzle, and the results are presented in **Figure 1**a. For all of the PLA solutions, a rheological shear-thinning behavior was observed, since the process-related apparent viscosity decreased with increasing process-related apparent shear rate. This property enhances the material processability during extrusion through the capillary nozzle under high shear rates due to a decrease in viscosity. Figure 1a also shows that the process-related apparent viscosity increased significantly with polymer content. The 30 wt% PLA solution was successfully used to fabricate 3-D freeform structures because of its relatively high viscosity, while the 25 wt% PLA solution was more suitable for 2D conformal printing. As for the 20 wt% PLA solution, it was difficult to form continuous smooth filaments for all the nozzles used (inner diameter ranging from 510 to 100 μm).

After filament extrusion of self-supporting features, the solvent evaporation plays a crucial role in the geometric retention. Upon rapid evaporation, the rigidity of the material significantly increases and provides the required structural support for the

deposition in a continuous manner and along different directions, therefore allowing freeform writing in open air. The solvent evaporation rate was investigated by monitoring the weight reduction of the deposited filament as a function of time using a high-precision balance. Figure 1b shows the solvent content evolution with time of a short filament (length of ~5 mm) deposited using a 510 μm inner diameter nozzle. The initial solvent fraction measured by our gravimetric method was smaller than the nominal content in the polymer solution. This lower value was attributed to the flash evaporation caused by rapid pressure reduction that occurs near the extrusion point.[26] Our results reveal that approximately 50% of the solvent evaporated within the first 3 minutes of the gravimetry test, and the filament deposited from the 30 wt% PLA solution exhibited the shortest drying period. Actually the utilization of a nozzle with an inner diameter of 100 μm was required to build 3-D freeform structures using the 30 wt% PLA solution. The solvent present inside a smaller diameter filament takes less time to diffuse to its surface and the rigidity of the filament increases more quickly, which is of great benefit to the 3-D geometric retention. During our process mapping, we observed poor 3-D freeform geometric retention when using the 30 wt% PLA solution and larger nozzles (≥ 200 μm), or using lower PLA content solutions (25 or 20 wt%) for all nozzles investigated.

Different kinds of 3-D microstructures were fabricated by the SC-DW assembly including a square spiral, circular spiral, micro-cup and 9-layer scaffold showed in **Figure 2**b-f. This flexible method enabled the fabrication of unique structures that are generally difficult to produce by conventional single-stage processing methods,

including floating (Figure 2b and c), spanning (Figure 2d and e) and scalable (Figure 2f) structures. Figure 2a shows top and isometric side views from a computer-aided design (CAD) image of the programmed deposition path of the SC-DW apparatus to manufacture a square spiral using eight 1.0 mm side length loops and a pitch of 0.7 mm. Figure 2b shows scanning electron microscopy (SEM) top and side view images of the actual square spiral deposited. The average side length of the actual square spiral was 1102 ± 15 μm and the average pitch was 707 ± 22 μm. For the circular spiral of Figure 2c, the average spring diameter was 966 ± 6 μm and the average pitch was 530 ± 25 μm. Both values were very close to the programmed deposition path (*i.e.*, spring diameter of 1.0 mm, pitch of 500 μm). The layer-by-layer scaffold (Figure 2d, e) and the micro-cup (Figure 2f) were almost identical to their respective programmed deposition paths because the printing layer was supported by the underlying layer. Consequently, the SC-DW method was demonstrated to be a flexible and high fidelity micromanufacturing process. The main limitation remains the freeform deposition of sharp turns which lead to some geometric discrepancies. For example, the measured average radius of the square spiral turn was 345 ± 7 μm, which was almost twice the programmed value (167 μm).

Three different microsystems were fabricated in order to demonstrate the fabrication capabilities of SC-DW. First, a high-toughness microstructured fiber was developed by harnessing a flow instability during the fabrication process. This application was inspired by the molecular structure of spider silk proteins.[27] The sacrificial bonds in the microstructured fiber play an analogous role to that of the

hydrogen bonds present in the molecular structure of the silk protein which give its toughness to spider silk.[27] **Figure 3**a shows a regular straight fiber and its neatly circular cross-section. Figure 3b displays a microstructured fiber fabricated by extruding the polymer solution towards a substrate moving perpendicularly at a slower velocity than the filament linear flow rate (see Supporting Information, Figure S1). The filament repetitively buckles giving rise to periodic meanders and stitch patterns. Uniaxial tension tests performed on the fibers reveals that the microstructured fiber exhibits a much higher breaking strain (straight fiber 116% vs. microstructured fiber 766%, Figure 3-D) due to the sacrificial bonds created when the viscous filament loops over itself and fuse. In order to stretch the fiber under uniaxial tension, the sacrificial bonds must be broken (see the stretched microstructured fiber in Figure 3c), hence adding to the total energy required for breaking the fiber.

Second, the SC-DW approach can also be used to fabricate complex microfluidic devices by using the printed thermoplastic features as a sacrificial material. As an example, we developed a 3-D microchannel that can be used for fluidic mixing[4] or particle separation.[28] Figure 3e shows fluorescent microscope top and side view images of the fluid-filled microchannel. This microfluidic channel was achieved by first depositing by SC-DW technique a freeform PLA spiral containing a catalyst.[29] After its encapsulation in epoxy and complete curing, the sample was heated in a vacuum oven in order to depolymerize the PLA and create a smooth microfluidic channel (see Supporting Information, Figure S2). Further optimization of the channel size and topological structures is ongoing for its incorporation into a highly efficient

micro-particles separator.

Finally, the SC-DW method also offers a new possibility to build electrically conductive structures such as high frequency devices. For instance, a small spiral Ka band antenna (20-30 GHz) was fabricated by depositing a PLA spiral featuring variable pitch distances followed by the sputtering of a ~50 μm copper layer coating. Figure 3f shows optical microscopy images of the metallic coated and PLA core small antenna. The measured current with respect to the applied voltage curve showed a nearly linear response within the voltage range investigated, and the calculated electrical resistance of the antenna was ~0.174 Ω (Figure 3g). More work is ongoing to characterize the spiral antenna and improve its telecommunication performance.

In summary, the SC-DW technique developed in this work offers a low-cost, highly flexible and powerful fabrication route for microsystems featuring mechanical, microfluidic and/or electrical functionalities. This technique represents an important step toward sustainable development for the microfabrication community due to its compatibility with recyclable and biodegradable materials (*e.g.*, PLA) and the very small production of waste materials even during the creation of complex 3-D freeform shapes. The extension of the fabrication capabilities of the technique could be achieved through the utilization of other inks (*e.g.*, bio-based and synthetic thermoplastics, electrically-conductive and mechanically-adaptive nanocomposites) and the printing of features at the submicron and potentially nanoscale. On a longer term, we envision that the SC-DW approach could be used in medicine (*e.g.*, printing of biocompatible and/or biodegradable 3-D micro-prosthetics, tissue engineering scaffolds or cylindrical mesh

for stents), in microelectronics (*e.g.*, inductance components, flexible electrical connections) and in structural composites (*e.g.*, microstructured fibers).

Experimental Section

Ink preparation: Neat polylactide (PLA 4032D, Natureworks LLC) was dissolved in dichloromethane (DCM, Sigma-Aldrich) to prepare polymer solutions with different PLA concentrations (20, 25 and 30 wt%). After resting for 12 h, the solutions were stirred and sonicated in an ultrasonic bath (Ultrasonic cleaner 8891, Cole-Parmer) for 1 h. The solutions were stored in sealed bottles until processing.

Capillary flow analysis: The process apparent viscosities of the three PLA solutions (20, 25 and 30 wt% PLA) were calculated from constant-pressure capillary flow data as described by Bruneaux *et al.*[30] The polymer solution was extruded through a micronozzle with an inner diameter of 200 μm (5127-0.25-B, EFD). After reaching the extrusion steady state, lines of ink were deposited onto a substrate for 60 s under eight applied pressures ranging from 0.2 to 3.5 MPa at a robot velocity of 1 mms^{-1}. The extruded fibers were dried in an oven (G05053-10, Cole-Parmer Instrument Company) at 50 ºC for 12 h and then weighed using a high-precision balance (GH-202, A&D Engineering Inc.). The mass of the fibers served to determine the mass flow rate, which was converted to the volumetric flow rate using the respective fluid densities. The capillary data reported in this work include the Rabinowitch correction. The Bagley correction for end effects was neglected because the ratio of the extrusion nozzle length to its diameter was larger than 50.

Determination of solvent evaporation rate: The solvent evaporation behavior of the polymer ink was evaluated by directly depositing a filament on a glass substrate resting on a high-precision balance. The computer controlled robot (I&J2200-4, I&J Fisnar) was used to deposit the polymer solutions on the substrate for 5 seconds through a nozzle with 510 μm (5121-0.25-B, EFD) inner diameter, under an applied pressure of 420 kPa. The sample weight change was recorded for 6 h. Following this recording period, the sample was completely dried in an oven at 50 ºC for 12 h and weighted again. The mass of the dried PLA was then used to calculate the solvent percentage in the deposited filament.

SC-DW assembly of 3-D structures: The deposition system consisted of a computer controlled robot (I&J2200-4, I&J Fisnar) moving a dispensing apparatus (HP-7X, EFD) along the *x*, *y* and *z* directions. The square spiral, circular spiral and micro-cup were fabricated with the 30 wt% PLA solution using a micronozzle with a 100 μm inner diameter (5132-0.25-B, EFD) under an applied pressure of 1.75 MPa and 0.1 mms^{-1} robot velocity. The pitch of the square spiral was 0.7 mm and the side length of the coil was 1.0 mm. The pitch of the circular spiral was 0.5 mm and the radius of the coil was 0.5 mm. The 9-layer scaffold was fabricated with the 25 wt% PLA solution using the 100 μm inner diameter nozzle under an applied pressure of 1.4 MPa and 1.0 mms^{-1} robot velocity. The filament diameter in the scaffold was about 80 μm and the inter-distance between two adjacent filaments was 500 μm.

Fabrication and characterization of high-toughness fiber: The microstructured fiber was fabricated by extruding the 26 wt% PLA solution through a 30 μm inner

diameter nozzle under an applied pressure of 0.7 MPa and 2.0 mm s^{-1} robot velocity. The tensile tests were performed using a dynamic mechanical analyzer (DMA Q800, TA Instruments). The load was increased at a rate of 0.5 N min^{-1} until the fiber was broken.

Fabrication of spiral microchannel: The channel was fabricated by first depositing the 30 wt% PLA solution with catalyst Tin(II) Oxalate (1.5 wt%, Sigma-Aldrich) into a circular spiral on a glass substrate. The deposited pattern was then encapsulated by pouring uncured epoxy (Epon 862/ Epikure 3274, Momentive) followed by its complete curing. The cured epoxy block was released from the glass substrate and cut in order to open the two ends of the microchannel. The sample was then heated in a vacuum oven at a temperature of 200 °C and an absolute pressure of 0.1 inHg for 48 h. This heat and pressure cycle depolymerized the PLA and left an empty microchannel in the epoxy.

Fabrication and characterization of antenna: A freeform circular spiral was created using a ~30 wt% PLA solution extruded through a 200 μm micronozzle diameter and a robot velocity of 0.1 mm s^{-1}. The 3-D antenna was completed by sputtering the PLA spiral with a ~50 μm copper layer coating using an electrolytic bath. The designed antenna featured eight coils for a total height of 23.2 mm and an internal diameter of 3.4 mm. The electrical conductivity of the antenna was measured with a laboratory DC power supply (GPS-3303, Instek) and a shielded I/O connector block (SCB-68, NI).

Morphological characterization: The microstructures were sputtered with gold for

15 s and observed on a Scanning Electron Microscope (SEM) (JSM-7600F, JEOL. Ltd.). The optical and fluorescent images were acquired with an optical microscope (BX-61, Olympus) and analyzed with image processing software (Image-Pro Plus 6.0, Media Cybernetics).

Supporting Information is available on the WWW under http://www.small-journal.com or from the author.

Acknowledgements

The authors acknowledge the financial support from NSERC (Natural Sciences and Engineering Research Council of Canada). A scholarship for Mr. Guo was also provided by the China Scholarship Council (CSC).

Received: ((will be filled in by the editorial staff))
Revised: ((will be filled in by the editorial staff))
Published online: ((will be filled in by the editorial staff))

[1] R. D. Farahani, H. Dalir, V. L. Borgne, L. A. Gautier, M. A. E. Khakani, M. Lévesque, D. Therriault, *Nanotechnology* **2012**, *23*, 085502.
[2] X. Xiao, L. Yuan, J. Zhong, T. Ding, Y. Liu, Z. Cai, Y. Rong, H. Han, J. Zhou, Z. L. Wang, *Adv. Mater.* **2011**, *23*, 5440.
[3] J. Yeom, M. A. Shannon, *Adv. Funct. Mater.* **2010**, *20*, 289.
[4] D. Therriault, S. R. White, J. A. Lewis, *Nat. Mater.* **2003**, *2*, 265.
[5] L. Y. Yeo, H.-C. Chang, P. P. Y. Chan, J. R. Friend, *Small* **2011**, *7*, 12.
[6] A. R. Hamilton, N. R. Sottos, S. R. White, *Adv. Mater.* **2010**, *22*, 5159.
[7] B. J. Blaiszik, S. L. B. Kramer, M. E. Grady, D. A. McIlroy, J. S. Moore, N. R. Sottos, S. R. White, *Adv. Mater.* **2012**, *24*, 398.
[8] A. P. Esser-Kahn, N. R. Sottos, S. R. White, J. S. Moore, *J. Am. Chem. Soc.* **2010**, *132*, 10266.
[9] K. S. Toohey, N. R. Sottos, J. A. Lewis, J. S. Moore, S. R. White, *Nat. Mater.* **2007**, *6*, 581.
[10] F. Klein, B. Richter, T. Striebel, C. M. Franz, G. v. Freymann, M. Wegener, M. Bastmeyer, *Adv. Mater.* **2011**, *23*, 1341.
[11] S. M. Berry, S. P. Warren, D. A. Hilgart, A. T. Schworer, S. Pabba, A. S. Gobin, R. W. Cohn, R. S. Keynton, *Biomaterials* **2011**, *32*, 1872.
[12] T. G. Leong, A. M. Zarafshar, D. H. Gracias, *Small* **2010**, *6*, 792.
[13] A. Yamada, F. Niikura, K. Ikuta, *J. Micromech. Microeng.* **2008**, *18*, 025035.
[14] T. D. Brown, P. D. Dalton, D. W. Hutmacher, *Adv. Mater.* **2011**, *23*, 5651.
[15] T. Yang, D. Wu, L. Lu, W. Zhou, M. Zhang, *Polym. Compos.* **2011**, *32*, 1280.

[16] C. A. Bonino, K. Efimenko, S. I. Jeong, M. D. Krebs, E. Alsberg, S. A. Khan, *Small* **2012**, *8*, 1928.
[17] J. A. Lewis, G. M. Gratson, *Mater. Today* **2004**, *7*, 32.
[18] D. Therriault, R. F. Shepherd, S. R. White, J. A. Lewis, *Adv. Mater.* **2005**, *17*, 395.
[19] G. M. Gratson, M. Xu, J. A. Lewis, *Nature* **2004**, *428*, 386.
[20] J. E. Smay, G. M. Gratson, R. F. Shepherd, J. Cesarano, J. A. Lewis, *Adv. Mater.* **2002**, *14*, 1279.
[21] B. Y. Ahn, D. Shoji, C. J. Hansen, E. Hong, D. C. Dunand, J. A. Lewis, *Adv. Mater.* **2010**, *22*, 2251.
[22] J. J. Adams, E. B. Duoss, T. F. Malkowski, M. J. Motala, B. Y. Ahn, R. G. Nuzzo, J. T. Bernhard, J. A. Lewis, *Adv. Mater.* **2011**, *23*, 1335.
[23] J. N. Hanson Shepherd, S. T. Parker, R. F. Shepherd, M. U. Gillette, J. A. Lewis, R. G. Nuzzo, *Adv. Funct. Mater.* **2011**, *21*, 47.
[24] R. A. Barry, R. F. Shepherd, J. N. Hanson, R. G. Nuzzo, P. Wiltzius, J. A. Lewis, *Adv. Mater.* **2009**, *21*, 2407.
[25] L. L. Lebel, B. Aissa, M. A. El Khakani, D. Therriault, *Adv. Mater.* **2010**, *22*, 592.
[26] Z. Gou, A. J. McHugh, *J. Non-Newtonian Fluid Mech.* **2004**, *118*, 121.
[27] N. Becker, E. Oroudjev, S. Mutz, J. P. Cleveland, P. K. Hansma, C. Y. Hayashi, D. E. Makarov, H. G. Hansma, *Nat. Mater.* **2003**, *2*, 278.
[28] J. Zhu, X. Xuan, *Biomicrofluidics* **2011**, *5*, 024111.
[29] H. Dong, A. P. Esser-Kahn, P. R. Thakre, J. F. Patrick, N. R. Sottos, S. R. White, J. S. Moore, *ACS Appl. Mater. Interfaces* **2012**, *4*, 503.
[30] J. Bruneaux, D. Therriault, M. C. Heuzey, *J. Micromech. Microeng.* **2008**, *18*, 115020.

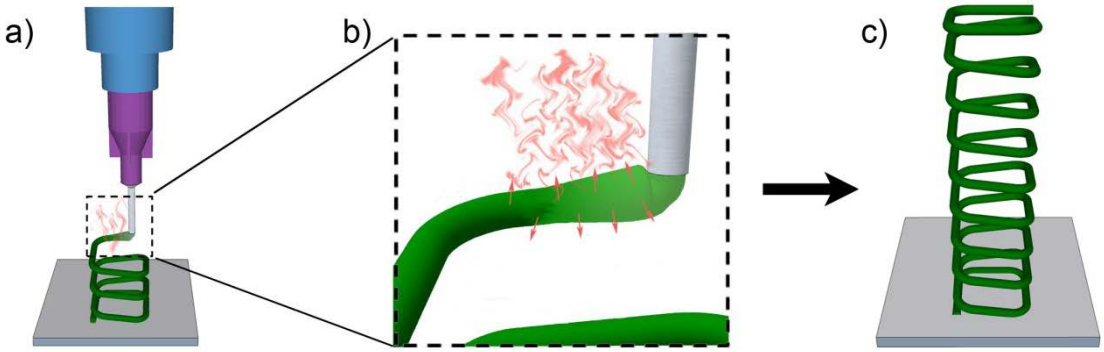

Scheme 1. Schematic representation of the SC-DW process with a thermoplastic solution. a) Deposition of the polymer solution through a micronozzle. b) Rapid solvent evaporation post extrusion. c) Example of a 3-D square spiral fabricated by the SC-DW assembly.

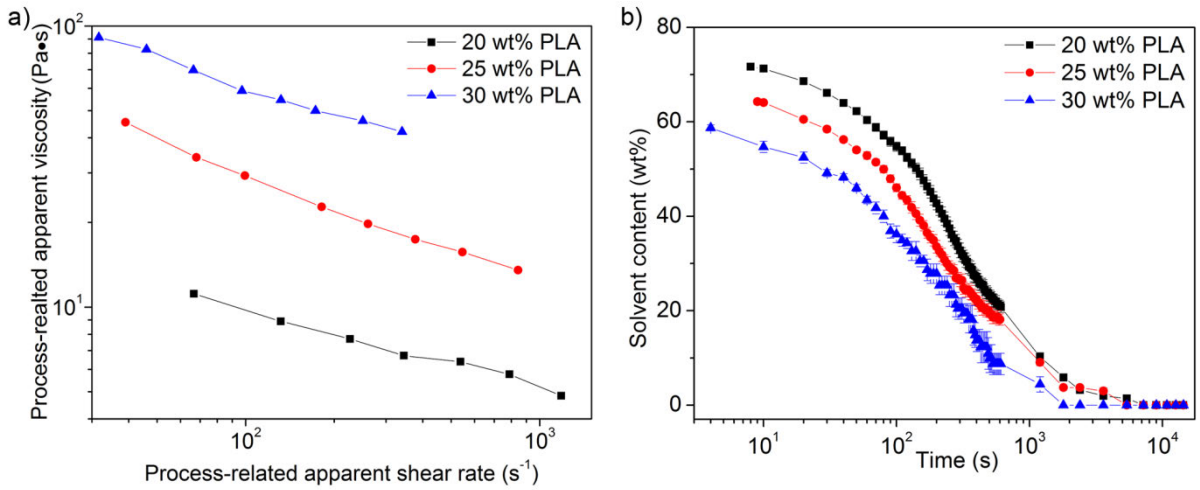

Figure 1. SC-DW ink characterization. a) Process-related apparent viscosity. b) Solvent content as a function of time for different polymer concentrations.

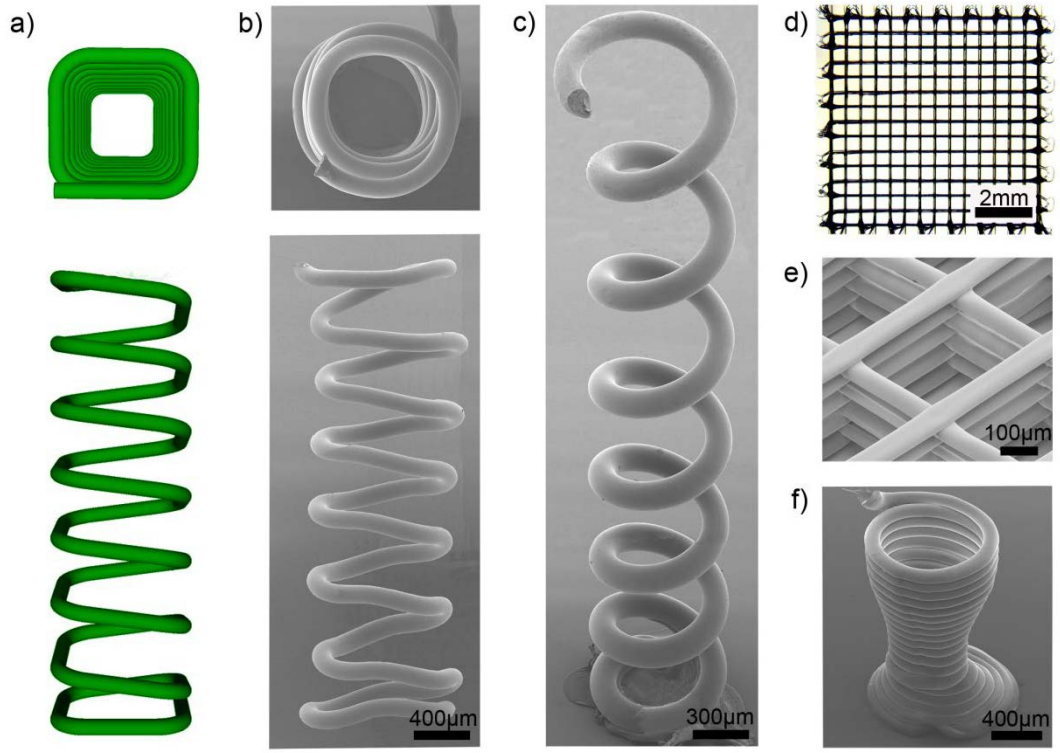

Figure 2. Microstructures manufactured by SC-DW. (a) Top and side view virtual images of the programmed SC-DW fabrication of the square spiral. (b) Top and side view SEM images of an actual PLA square spiral. (c) Inclined top view SEM image of a PLA circular spiral. (d) Representative optical image of a PLA scaffold composed of nine layers. (e) Inclined top view SEM image of PLA 9-layer scaffold. (f) SEM image of a PLA cup.

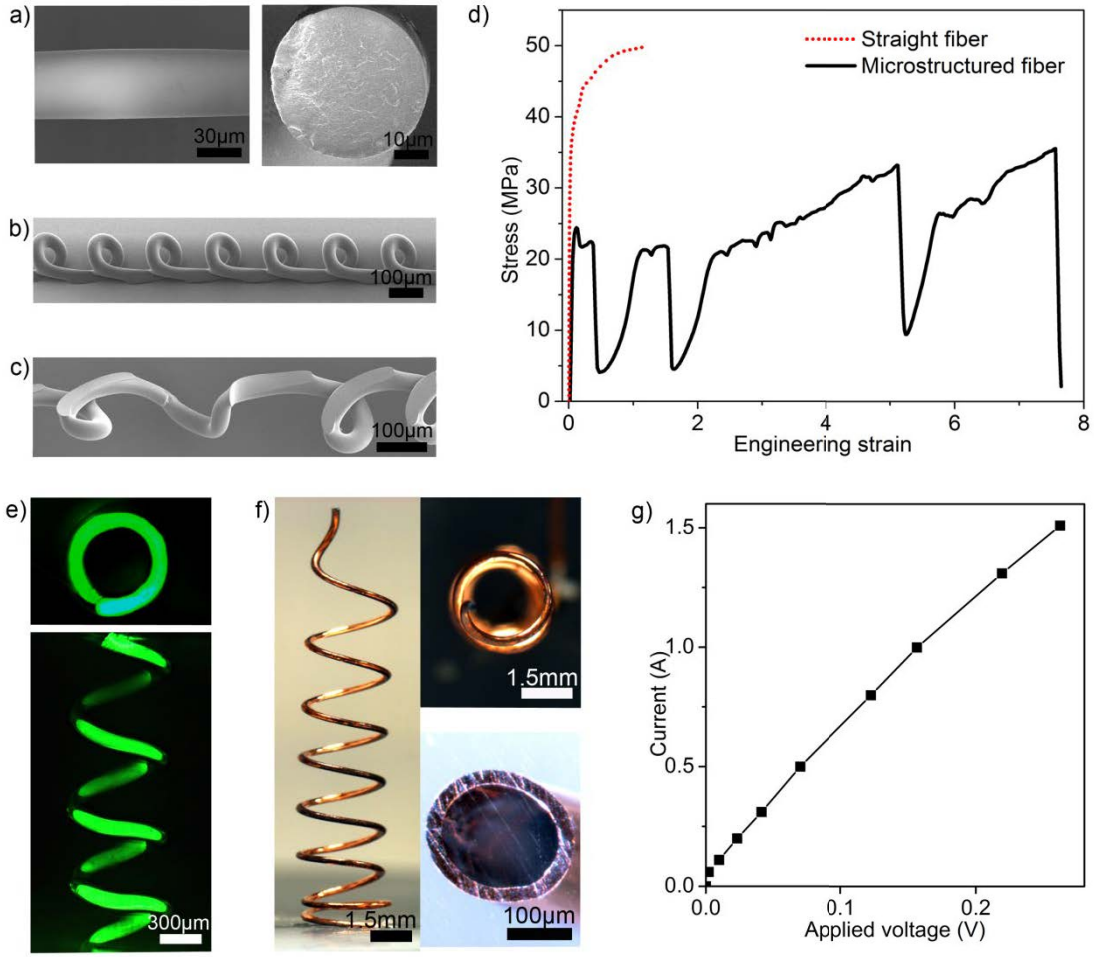

Figure 3. Representative SEM images of a) straight PLA fiber and its circular cross section, b) microstructured PLA fiber with sacrificial bonds, and c) stretched microstructured fiber. d) Tensile properties comparison for a straight fiber (dash line) and a microstructured fiber (solid line). e) Fluorescent microscopy top and side view images of a fluid-filled spiral microchannel embedded inside an epoxy matrix. f) Optical side, top and cross-sectional view images of the copper coated 3-D variable pitch spiral antenna. g) Measured current upon voltage application between two ends of the 3-D spiral antenna.

The table of contents

The solvent-cast direct-write fabrication of microstructures is shown using a thermoplastic polymer solution ink. The method employs the robotically-controlled micro-extrusion of a filament combined with a rapid solvent evaporation. Upon drying, the increased rigidity of the extruded filament enables the creation of complex freeform 3-D shapes.

Microfabrication, solvent evaporation, polymer solution, polylactide, 3-D Printing

Shuang-Zhuang Guo, Frédérick Gosselin, Nicolas Guerin, Anne-Marie Lanouette, Marie-Claude Heuzey and Daniel Therriault*

Solvent-Cast Three-Dimensional Printing of Multifunctional Microsystems.